Ab Initio Evaluation of Uranium Carbide $S(\alpha,\beta)$ and Thermal Neutron Cross Sections

Jonathan Crozier[1*], *Ayman* Hawari[1]

[1]Department of Nuclear Engineering, North Carolina State University, Raleigh NC 27695, USA

Abstract. Uranium Carbide (UC) is a nuclear fuel material which offers better neutron economy and lower fuel-cycle costs compared to conventional mixed-oxide fuels. UC's lattice binding and dynamical properties impact thermal neutron scattering and low temperature epithermal resonance absorption. The Thermal Scattering Law (TSL) describes the scattering system available energy and momentum transfer states. There is no TSL evaluation for UC in the ENDF/B-VIII.0 database; herein, *ab-initio* lattice dynamics (AILD) techniques are invoked to calculate the phonon spectrum for UC using spin-orbit-coupling density functional theory (DFT). The TSLs, inelastic and elastic thermal scattering cross sections for Uranium and Carbon in UC, respectively, are calculated in *FLASSH* for use in higher fidelity reactor design calculations.

Introduction

Uranium Carbide (UC) is a nuclear fuel material, whose crystal binding may affect thermal and epithermal neutron interactions. Currently, there is no Thermal Scattering Law (TSL) evaluation for UC in the ENDF/B-VIII.0 database. *Ab-initio* lattice dynamics (AILD) techniques are used to calculate the phonon spectrum using spin-orbit-coupling density functional theory (DFT). The calculations herein detail the TSL evaluations for Uranium and Carbon, respectively, in UC, and their thermal neutron scattering cross sections.

1.1 Thermal Scattering Law Theory

The thermal neutron de-Broglie wavelength is on the order of magnitude of inter-atomic spacing and its energy is on the order of magnitude of lattice vibrations. The thermal scattering interactions in a crystalline material are therefore a function of structure and vibrational mode availability: inelastic scattering energy can be transferred to absorption and emission of elementary excitations (phonons), and elastic scattering occurs at Bragg edges. The double differential thermal scattering cross section is proportional to the thermal scattering law, $S(\alpha,\beta)$:

$$\frac{\partial^2\sigma}{\partial\mu\partial E'} = \frac{1}{2k_BT}\sqrt{\frac{E'}{E}}\left(\sigma_{coh}S(\alpha,\beta) + \sigma_{inc}S_s(\alpha,\beta)\right) \quad (1)$$

$$S(\alpha,\beta) = S_s(\alpha,\beta) + S_d(\alpha,\beta) \quad (2)$$

where μ is the scattering angle cosine, E and E' are respectively incident and outgoing neutron energies, T is the temperature, k_B is the Boltzmann constant, σ_{coh} and σ_{inc} are respectively coherent and incoherent bound cross sections, and S is the TSL as a function of dimensionless momentum and energy transfer variables α and β [1,2].

The differential cross section is therefore a summation of interference (coherent) and non-interference (incoherent) contributions. The space-time correlation of atomic position with its initial position is described by the *self* component of the TSL, $S_s(\alpha,\beta)$, and the correlation with surrounding atoms described by the *distinct* effects, $S_d(\alpha,\beta)$ [1].

The scattering law can be calculated in a phonon expansion assuming harmonic lattice forces, where the 0^{th}-order contribution (no phonon exchange) details elastic scattering, and the summation of n^{th}-order contributions (phonon creation / annihilation) describe inelastic scattering.

Several assumptions can be made to improve the computational feasibility of a TSL evaluation. The incoherent approximation assumes negligible *distinct* contributions to inelastic cross section and the cubic approximation assumes that energy and momentum transfer are independent of lattice directionality. These approximations can be reasonable depending on the elemental and structural configuration of the evaluated scattering system.

1.2 Computational Methods

UC has a rock-salt crystal structure with Fm-3m symmetry (space group 225). Highly correlated semi-itinerant bonding and magnetic ordering exists for Uranium's *5f* electrons [3,4].

Structure minimization for Uranium Carbide's anti-ferromagnetic (AFM) ground state was conducted with

* Corresponding author: jpcrozie@ncsu.edu

VASP code using spin-orbit-coupling (SOC) [5] which invoked PAW pseudo-potentials with the GGA-PBEsol exchange-correlation functional [6]. A Methfessel-Paxton smearing width of 0.2 eV was used [7], and an effective Hubbard value (U-J) controlled the degree of Uranium 5*f* electron itineracy [8]. Additionally, the plane wave cut-off [9] and Monkhorst-Pack k-mesh [10] ensured sufficient convergence of ground state energy and volume.

A 2x2x2 cubic supercell calculation (64 atoms) displaced non-equivalent U and C atom sites by 0.02 Å in ± x-direction. The UC isotropic magnetic phase was approximated by weighting Hellman-Feynman forces for AFM-I ordering along perpendicular (001) and parallel (100) planes with respect to atomic displacements [11.

Phonon dispersion relations and partial phonon DOS were generated in the PHONON code[12] by solving for the eigenvalues of the dynamical matrix. The partial DOS for Carbon and Uranium were processed in *FLASSH* [13] to generate their respective TSL data, incoherent inelastic and coherent elastic cross section data. These calculations assume isotropic compositions of U and C. The free atom cross sections and masses correspond current ENDF data [14]. The total cross section for UC can be compared to experimental transmission data by accounting for the Uranium absorption cross section.

2 Results and Discussion

2.1 *Ab Initio* Structure and Lattice Dynamics

The VASP DFT Framework's prediction of minimum energy structure demonstrates excellent agreement with the experimental lattice parameter in Table 1. The under-estimation is consistent with similar *DFT+SOC+U* frameworks [15], and is necessary for an accurate, non-degenerate description of Carbon phonon dispersion modes which are highly sensitive to Uranium's 5*f* interactions

Table 1. Calculated Lattice Parameter for UC.

Lattice Constant	DFT	Experiment [16]	% Deviation
Å	4.9275	4.960	-.0654

The predicted electronic DOS is in reasonable agreement with experimental x-ray photoemission spectroscopy (XPS) and bremsstrahlung isochromat spectroscopy (BIS) data [17] centred at the fermi energy. This suggests that the present model may accurately represent 5*f* behaviour and nearest neighbour atomic forces.

In Figure 1, UC's phonon dispersion relation is compared with inelastic neutron scattering (INS) data [18]. Carbon's vibrational states primarily dominate the high energy longitudinal and transverse acoustic modes (LA,TA), whereas Uranium's states dominate the longitudinal and transverse optical modes (LO,TO). The anticipated lack of Γ-point LO/TO splitting, and non-degenerate LA/TA trajectories in the [ξξξ] direction demonstrate excellent agreement with experimental data.

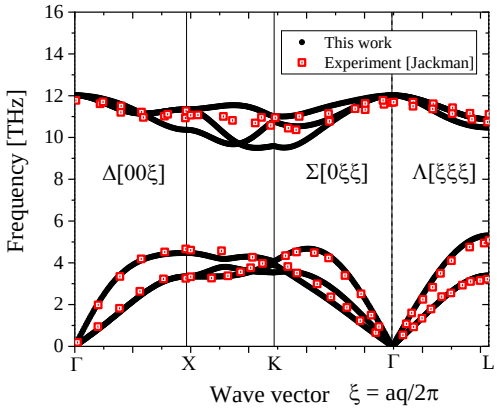

Fig 1. UC Phonon Dispersion Relations compared with Experimental INS Data

The neutron-weighted, generalized phonon spectrum further demonstrates good agreement with time of flight (TOF) measurements [19], as per Figure 2. Oxygen impurities in the experimental sample introduce additional phonon states around 0.03 eV. The low energy phonon peaks are dominate by Uranium contributions, and the high energy peaks are dominated by the Carbon dynamical contribution. The partial phonon DOS are depicted in Figure 3.

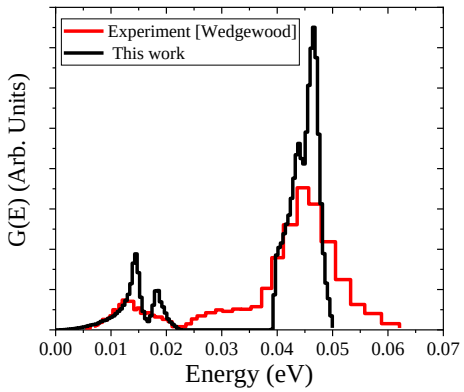

Fig 2. UC Phonon DOS Relations compared with Experimental TOF Data

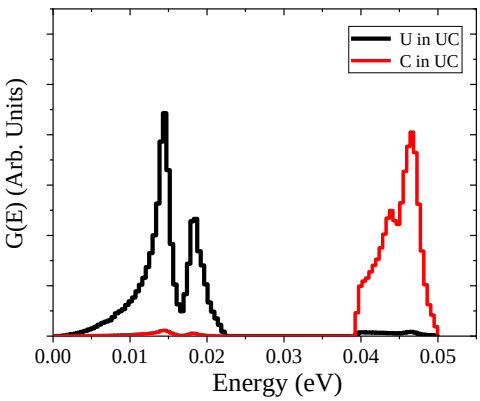

Fig 3. UC Partial Phonon DOS for U and C

2.2 Thermal Scattering Law

Uranium and Carbon's phonon DOS is used in *FLASSH* to evaluate their TSL data for temperatures between 296 K and 2000 K with a phonon order of 800. This high phonon order removes the need for the short-collision-time (SCT) approximation for large α and β. The TSL surfaces for Uranium and Carbon in Figures 4 and 5 carry the characteristics of their phonon spectra particularly for those β within the range of the DOS. The oscillatory nature of the Carbon TSL along β is characteristic of quantum harmonic behaviour.

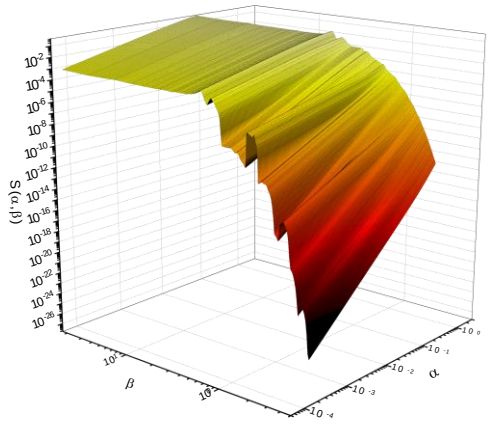

Fig 4. Uranium in UC TSL Surface at 296 K

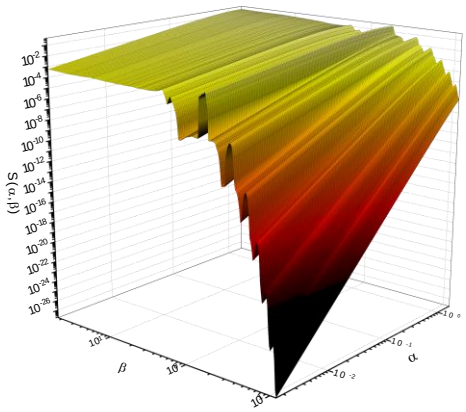

Fig 5. Carbon in UC TSL Surface at 296 K

2.3 Thermal Scattering Cross Sections

The incoherent inelastic and the coherent elastic cross sections calculated in *FLASSH* yield the total thermal scattering cross sections for U and C in UC, as presented below for 296, 600, 1200 and 2000 K in Figures 6 and 7.

Inelastic scattering dominates below 0.005 eV, after which characteristic elastic scattering peaks occur at Bragg edges. The total thermal scattering cross sections converges to respective free-atom cross sections. By additionally considering Uranium neutron absorption, the total UC cross section compares well with neutron transmission data [20] in Figure 8.

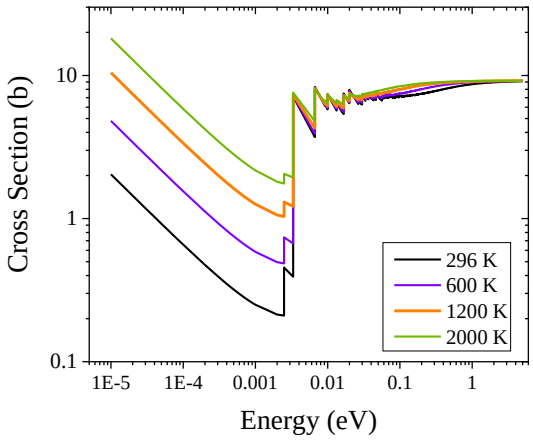

Fig 6. Uranium in UC total thermal scattering cross sections for varying temperatures

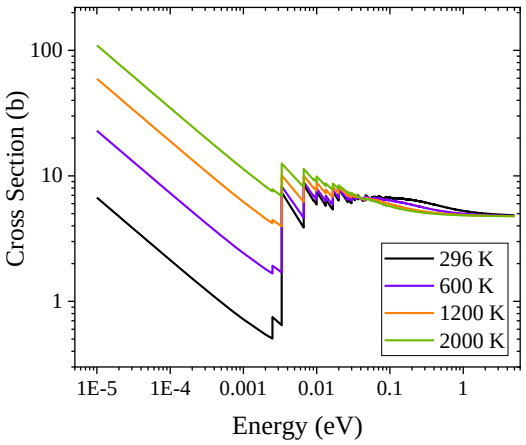

Fig 7. Carbon in UC total thermal scattering cross sections for varying temperatures

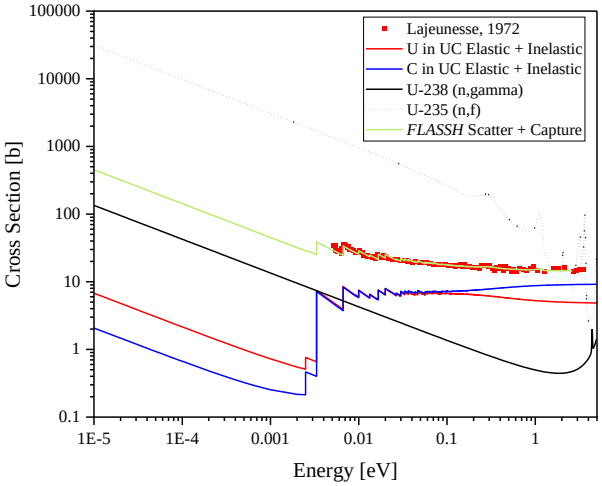

Fig 8. Coherent elastic, incoherent inelastic, absorption and total cross sections for UC at 296 K compared to neutron transmission data.

3 Conclusions

The TSL evaluation of Uranium and Carbon in UC invokes high-fidelity atomistic simulation which accurately accounts for Uranium's complex magnetic structure and semi-itinerant 5*f* orbital behavior; the predicted lattice parameter, electronic DOS, phonon dispersion relations, and generalized phonon DOS demonstrate excellent agreement with experimental data. Furthermore, the *FLASSH* code allows for first-principles production of coherent elastic, incoherent inelastic and TSL-broadened neutron absorption cross sections [21] which account for crystal binding effects on thermal neutron interactions.

This work was partially funded by the US National Nuclear Security Administration's (NNSA) Nuclear Criticality Safety Program (NCSP), and the US Naval Nuclear Propulsion Program (NNPP).

References

1. G. Squires, *Introduction to the Theory of Thermal Neutron Scattering*, Camb. Univ. Press, UK (1978)
2. A.I. Hawari, *Modern Techniques for Inelastic Thermal Neutron Scattering Analysis*, Nuc. Data Sheets 118 (2014)
3. T. Ohmichi, T. Saito, *Magnetic susceptibility of Uranium Carbonitride and Oxycarbide*, J. Nuc. Sc. and Tech., **8**(6) 314-318 (1971)
4. L. Bates, P Unstead, *The magnetic susceptibility of some carbides of uranium and thorium*, Br. J. Appl. Phys., **15** 543 (1964)
5. G. Kresse, D. Joubert, *From ultrasoft pseudopotentials to the projector augmented-wave method*, Phys. Rev. B **59**, 1785 (1999).
6. J. Perdew et al., *Generalized Gradient Approximation Made Simple*, Phys. Rev. Letters, **77** 18 (1996)
7. M. Methfessel, A. Paxton, *High-precision sampling for Brillouin-zone integration in metals*, Phys. Rev. B **40** (1989)
8. S. Dudarev et al., *Electron-energy-los spectra and structural stability of nickel oxide: an LSDA+U study,* Phys. Rev. B **57** (1998)
9. G. Kresse, J. Hafner, *Ab initio molecular dynamics for liquid metals*, Phys. Rev. B **47** 558 (1993)
10. H. J. Monkhorst and J. D. Pack, *Special points for Brillouin-zone integrations,* Phys. Rev. B **13** (1976).
11. J. L. Wormald et al., *Impact of Magnetic Structure and Thermal Effects on Vibrational Excitations and Neutron Scattering in Uranium Mononitride*, Annals of Nuclear Energy, **143** (2020).
12. K. Parlinski et al., *First-Principles Determination of the Soft Mode in Cubic ZrO 2*, Physical Review Letters, **78**, 4063 (1997).
13. N. Fleming et al., *FLASSH 1.0: Thermal Scattering Law Evaluation and Cross Section Generation for Reactor Physics Applications,* PHYSOR – Reactor Physics Paving the Way for More Efficient Systems," Proc. of PHYSOR (2022)
14. D. A. Brown et al., *ENDF/B-VIII.0 The 8th Major Release of the Nuclear Reaction Data Library with CIELO-project Cross Sections, New Standards and Thermal Scattering Data,* Nuclear Data Sheets **148** (2018).
15. U. Wdowik et al., *Effect of spin-orbit and on-site Coulomb interactions on the electronic structure and lattice dynamics of uranium mono-carbide*, Phys. Rev. B **40** (2016)
16. A. Padel, CH. Novion, *Constantes elastiques des carbures, nitrures et oxydes d'uranium et de plutonium*, J. of Nuc. Mat. **33** 1 (1969)
17. T. Ejima et al., *Studies of uranium compounds by photoemission and bremsstrahlung isochromat spectroscopy*, Physica B **186-188** (1993)
18. J. Jackman et al, *Systematic study of the lattice dynamics of the uranium rocksalt-structure compounds*, Phys. Rev. B **33** (1986)
19. F. Wedgewood, *Actinide chalcogenides and pnictides. III. Optical phonon frequency determination in UX and ThX compounds by neutron scattering*, J. of Phys. C: Solid State Physics **7**(18) (1974)
20. C. Lajeunesse et al., *Low Energy Neutron Interactions with Uranium Carbide*, Nuc. Sc. and Eng. **47**:3 (1972)
21. J.P.W. Crozier. N.C. Fleming, A.I. Hawari, *Thermal Scattering Law for Structure-Dependent-Doppler Broadening in FLASSH*, Proc. of PHYSOR (2022)